Structures 72 (2025) 108218

Contents lists available at ScienceDirect

Structures

journal homepage: www.elsevier.com/locate/structures

Multi-level response modification factor assessment in conventional and reduced length buckling-restrained braced frames

S. Ali Razavi *, Milad Ehteshami Moeini

Department of Civil Engineering, University of Science and Culture, Tehran, Iran

ARTICLE INFO

Keywords:
Buckling-Restrained Braced Frame (BRBF)
Reduced Core Length BRBs (RL-BRB)
Pushover analysis
Endurance Time Method (ETM)
Post-elastic stiffness

ABSTRACT

Buckling-restrained braced frames (BRBF) offer effective lateral resistance by preventing global buckling of the brace core under compression, resulting in symmetric hysteretic loops and efficient energy dissipation. However, despite enhanced cyclic performance compared to conventional braces, BRBs still lack sufficient post-yielding stiffness, leading to excessive drifts. Core length reduction effectively increases BRB stiffness without altering core cross-sectional area. Braced bay beam-to-column connections also influence BRBF lateral response. Nonlinear static and dynamic analyses were conducted on 4 buildings, including 4, 7, 9, and 12-story structures, with conventional and reduced core length BRBs (RL-BRB) in diagonal and chevron configurations. RL-BRBs with 20 % and 40 % core lengths were evaluated, considering hinged and rigid connections. A 4-story dual SMRF-BRBF was included for comparison. Results show RL-BRBFs exhibit superior lateral response, increasing seismic response modification factors by approximately 30 % in DBE level and 66 % in MCE level, with added benefits of being replaceable, repairable, and cost-efficient compared to conventional BRBFs.

1. Introduction

Buckling-restrained braced frames (BRBF) have been broadly acknowledged and used as an effective lateral resistance system in regions with high seismic hazards. BRBs are enhanced versions of conventional braces. Conventional braces tend to buckle when subjected to compressive axial loads. This phenomenon reduces the ultimate capacity of the brace; Thus, the size of the brace increases in the process of determining the proper cross-sectional area. Moreover, braced bay beam-columns and connections must be designed to be capable of resisting the yield capacity of the braces [1,2], resulting in an increase in their corresponding demands due to the increase in the brace size. These undesirable aspects sought researchers to improve the buckling behavior of conventional braces. The first attempts were carried out in Japan by proposing grout encasing for H section braces to improve the post-buckling behavior of the brace [3]. Though their efforts showed promise they failed to achieve optimum response due to the bond between the grout encasing and the steel H section which resulted in excessive stress in the restrainer. Further investigations were conducted to provide a proper debonding mechanism between the core plate and the encasing. These studies led to the introduction of the very first practical BRBs consisting of mortar infilled steel tube restraining the global buckling of the core plate [3]. BRBs behave almost symmetrically in both compression and tension. Such behavior indicates exceptional energy dissipation as opposed to conventional brace behavior. The great energy dissipation capability led many of the engineers to consider BRBs (also known as unbonded braces) as a type of hysteretic damper [4,5]. To ascertain the fussy performance of the BRBs research projects were conducted which concluded in design procedures [6]. BRBs can also be used in the seismic retrofit of steel and concrete structures [7,8]. To this day, several seismic analytical studies have been performed on BRBFs to evaluate their seismic response. A study by Tremblay et al. showed that short core BRBs can effectively decrease the drifts in the structure, nonetheless, it can drastically increase the induced stress in the restrainers [9].

In a study conducted by Kazemi and Jankowski incorporation SM in conventional BRBs was proposed and assessed as a solution to reduce the seismically induced residual drifts [10,11]. Other studies also paid attention to use machine learning in measuring the induced drifts and residual drifts in BRBFs by employing statistical indicators [12]. Recent studies proposed a new method for estimating median residual drifts of Buckling Restrained Braced Frames (BRBFs) by Asgarkhani et al., [13] named The coefficients method, which was calibrated for estimating the median of maximum residual drifts of BRBFs. The studies further

* Corresponding author.
E-mail addresses: arazavi@usc.ac.ir (S.A. Razavi), m.ehteshami.m@gmail.com (M.E. Moeini).

https://doi.org/10.1016/j.istruc.2025.108218
Received 22 October 2023; Received in revised form 10 October 2024; Accepted 7 January 2025

developed deflection amplification factors for the BRBFs to assure the proper mechanism of the structure [14].

Even though BRBFs have provided better lateral response compared to the conventional bracing systems, there are still concerning disadvantages that need further improvement. Investigations carried out on a prototype 4-story BRBF by Fahnestock et al. indicated satisfactory seismic performance, however, the results insinuated that the ductility demand is beyond that of considered in the design procedures [15]. The results of another study conducted by Merzouq and Tremblay on a multi-story BRBF located in Victoria, B.C. showed excessive seismic drifts [16]. The performance of the same structure was evaluated as satisfactory when designed along with a secondary lateral resistance system (i.e., dual SMRF-BRBF). The somewhat poor performance of BRBFs in certain cases was assumed to be caused by the low post-elastic stiffness especially when the braced bay beam-to-column connections were considered as pined [17,18]. Zaruma and Fahnestock assessed the collapse performance of BRBFs and the affecting parameters [19]. They noted that conventional BRBFs do not exhibit adequate overstrength and are prone to large drifts. They recommended dual SMRF-BRBF as a means to provide sufficient overstrength. To overcome the poor post-elastic stiffness, Razavi et al. proposed a method to increase the stiffness of the BRBs by reducing the core length [18]. The proposed Reduced Length BRB (RL-BRB) is made up of a BRB and an elastic HSS or Pipe brace, as depicted in Fig. 1. Experimental and numerical studies were conducted on RL-BRBs to assess their cyclic behavior [20]. The proposed RL-BRB proved to be effective in reducing the induced drifts and residual drifts due to the increased post-elastic stiffness of the dissipating units [21]. important to know the reason to incorporate reduced core lengths in BRBs. Buckling restrained braces improve the force capacity of the bracing system, on the other hand, they generally possess lower values of stiffness, while being cost-efficient. Hence, in cases the drift response of the structure cannot be controlled by the conventional BRBs the RL-BRBs are great solutions. Furthermore, due to the fact that fuse segment of the structure or the RL-BRB is smaller, the replicability of the fuses are greatly enhanced. Regarding the state of the art, several citations have been made which include response modification factor derivation for specific RL-BRBs which derived the response modification factors yet in much smaller scopes and neglecting some of the parameters assessed in this study. While the aforementioned articles derived response modification factors for the RL-BRBFs, the current study is far more inclusive by considering the braced bay beam connection influence, the dual action, variety of core lengths and different seismic intensities though ET method. Another very important factor which have been neglected before in previously conducted research is the decreased ultimate strain capacity of the RL-BRBs due to fatigue (which was derived from experimental results as cited in the literature) which play a very important role on determining the response parameters.

2. Research novelty

Performance-based design (PBD) in structural engineering aims to evaluate a structure's behavior across diverse loading scenarios, ensuring it meets specific performance criteria such as safety, functionality, and resilience, rather than solely adhering to fixed code requirements. PBD offers a more customized and efficient approach to structural design, taking into account factors such as material properties (ultimate strain capacity), seismicity, and occupancy to enhance performance and mitigate risks. In this study, a performance-based assessment was conducted by considering a wide array of influential factors and structural configurations while evaluating the structure's response to various seismic intensities, thereby assisting engineers in integrating PBD more effectively into RLBRBF systems. In order to comprehensively evaluate the seismic response of Reduced Length Buckling Restrained Braced Frames (RL-BRBFs), a series of structures ranging from 4 to 12 stories were considered, with combinations of inverted V braced frames in one direction and diagonal braced frames in the other. The brace lengths in each frame were varied to correspond to 100 %, 40 %, and 20 % of the total brace lengths. Both hinged and fixed connections for the braced bays were examined for each frame. Additionally, a 4-story frame with dual bracing was included, resulting in a total of 49 frames designed and analyzed.

All frames underwent analysis under monotonic static loads as well as intensifying time history. The dynamic analyses utilized the Endurance Time Method (ETM) as proposed by Estekanchi et al. This method involves subjecting structures to specially designed accelerograms, determining their Endurance Time (ET) based on their ability to withstand the dynamic forces applied during the process. The procedure for generating uniform ET accelerograms that meet code requirements is outlined in [17], with a specific set of three accelerograms employed in the analysis of moment and braced steel frames.

The noteworthy new aspects of the research are as follows:

- The current design guides focus on specific seismic intensity levels, whereas the performance base design (PBD) procedures consider a wide range of intensities. Due to the fact that the design response

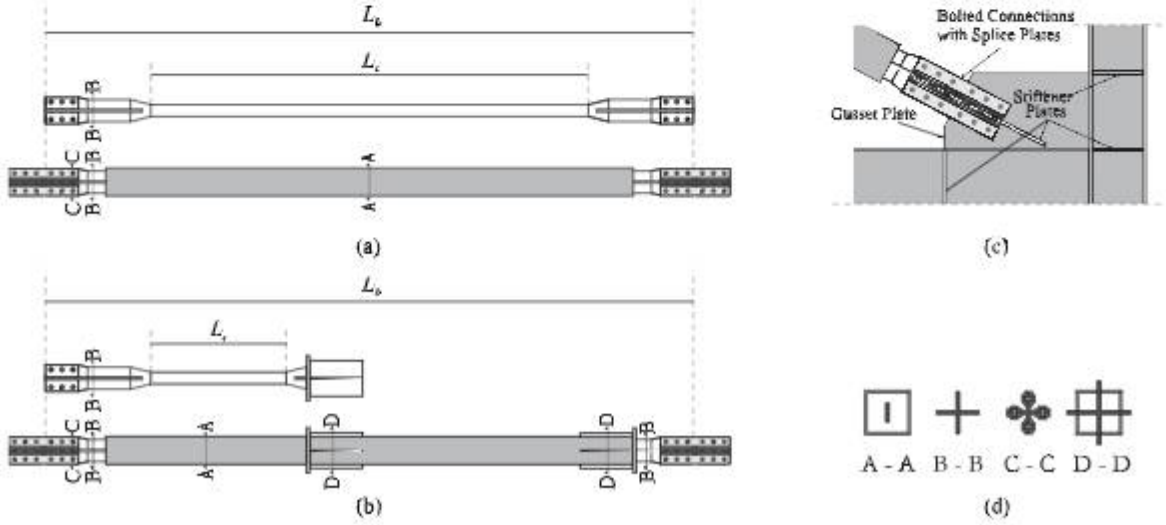

Fig. 1. Buckling-restrained brace in conventional and reduced core length configurations; (a) Conventional BRB, (b) RL-BRB, (c) Gusset details; and (d) cross sections.

modification factor is demand based, the currently available response modification factors as well as other response parameters are prone to imprecise design results. In this study the structural response parameters are derived in a variety of seismic intensities and can help structural engineers and researchers in regards to PBD procedures.

- Previous studies have examined fixed brace bay beams, RLBRBs with varying yielding segment lengths, and diagonal and chevron configurations. However, they did not compare these variables interactively or within a performance-based design (PBD) framework across different seismic intensities. The influence of each of the mentioned variables on the seismic response parameters is studied in this investigation.
- Though studies were carried out to assess the seismic response of the RLBRB frames, this system has never been assessed before using the Endurance Time Method (ETM). Employing such a method will not only result in the derivation of values for Response parameters such as, overstrength, ductility factor and response modification factors for selected seismic excitation levels, but in fact, the method results in an extensive wide range of response parameters for varieties of earthquake levels. The comparative results are indeed useful to grasp a comprehensive understanding of the core length influence on seismic response of the RLBRBF systems. Moreover, the grand scheme of the analyses is a guarantee to minimum error. Various parameters and structural configurations were also included in the scope of the work, such as braced bay beam connection rigidity, various core lengths for BRBs, bracing configuration, and dual SMRF-BRBF systems. Overall, this study provides wide and extensive research regarding the RLBRBFs, hoping to help engineers and researchers to fully understand the proposed system

A detailed report was compiled and presented to facilitate comparison and achieve a comprehensive understanding of the seismic response exhibited by the proposed system. Overall, this study offers a comprehensive and extensive investigation of RLBRBFs, aiming to enhance engineers' and researchers' understanding of the proposed by considering the interaction of a wide range of varieties system. Such a thorough and inclusive study has not been conducted by researchers previously.

3. SEISMIC design of brbf buildings

3.1. Prototype buildings and seismic data

Though several numerical studies were conducted on lateral response of RL-BRBFs, there are still aspects that need to be investigated. In this study, nonlinear static and dynamic analyses are performed on 4, 7, 9 and, 12-story buildings with the plan dimensions of 30 m × 22.5 m, as illustrated in Fig. 2. The story height was assumed to be 3.5 m. Two diagonal BRBFs in the East-West direction and one chevron (Inverted V) BRBF in the North-South direction were considered. Each of the lateral resisting frames were designed with three BRB core lengths, i.e., conventional BRB and RL-BRB with core lengths of 20 % and 40 % of total brace length. Each of the frames were designed with both pined and rigid-end connections. The 4-story diagonally braced frame was also designed as dual SMRF-BRBF. The braced bay beam connections were considered as pined, while the middle bay beams (between the two braced bays) were considered as SMRF moment resisting beams, designed to be capable of withstanding 25 % of total base shear. In total, 49 frames were analyzed. The overall three-dimensional view of the buildings equipped with RL-BRBs is presented in Fig. 3.

The structural site location is assumed to be in the San Francisco bay area. The design is performed in accordance with ASCE 7–16 [23]. The roof and floor dead loads, as well as the weight of the exterior cladding are equal to 2.8, 3.4 and 0.75 kPa, respectively. The roof and floor live loads are equal to 1.0 kPa and 2.4 kPa, respectively. For seismic loading,

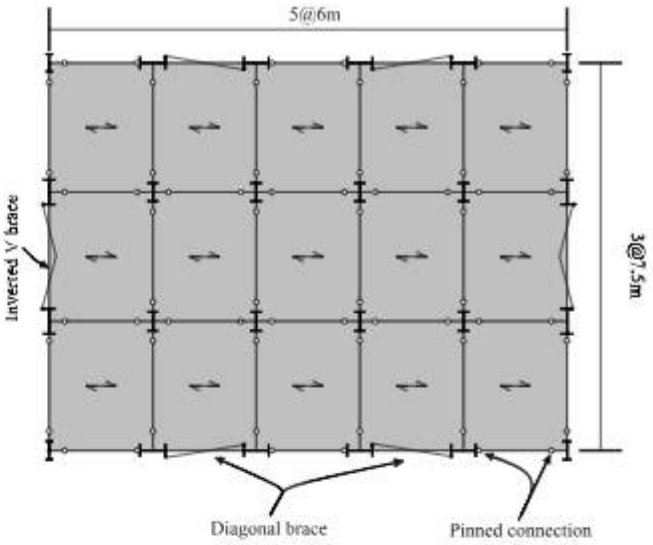

Fig. 2. Floor plan of the buildings.

it was assumed that the buildings are located on soil Type D with Fa = 1.0, Fv = 1.5 as per ASCE 7–16. The mapped maximum considered earthquake (MCER) spectral response acceleration parameters are S_S = 1.03 g at the short period and S_1 = 0.6 g at the 1.0 s period. The structure is assigned to the Seismic Design Category (SDC) E and the BRBF system with a response modification factor R = 8 is selected. The importance factor I_e is equal to 1. The fundamental periods, seismic mass, and the design base shears, are presented in Table 1. The design spectrum is illustrated in Fig. 4.

3.2. Seismic design of BRBFs

Several new studies have pointed out the proper amplification factors and drift control procedures for seismic design of BRBFs as previously mentioned in the literature review [13,14]. The studies emphasize on considering the resultant forces of the BRB cores on the boundary conditions. The design procure is explained in this section. The steel frame members are designed in accordance with the AISC 360–16 [24] Specification and the AISC 341–16 Seismic Provisions [1]. The cross-sectional areas of the BRB cores were selected to resist the design seismic base shear in tension and compression. ASTM A36 was selected as the BRB core material with a yield strength Fy = 262 MPa (reported by coupon tests). Beams and columns were selected from wide-flange sections conforming to ASTM A992 steel with Fy = 345 MPa. The same steel grade i.e., ASTM A992 was used for the elastic pipes. The force-controlled elements including beams and columns and in the case of RL-BRBs, the elastic pipe braces, were then designed to carry the expected forces resulting from the tensile or compressive yielding of the BRB cores. The beams with moment-resisting connections were designed to resist the combination of seismic and gravity-induced moments while considering the interaction with the seismic-induced axial force. The seismic induced axial forces of the force-controlled elements were derived using the procedure depicted in the free-body diagram in Fig. 5.

The amplification parameters of ω and ωβ (i.e., the tension and compression overstrength factors derived from the backbone curve of the BRBs) were calculated for each BRB using the expected elastic strain demand of the brace cores at each floor. The BRB core strain demand for each floor was calculated after preliminary analysis and design. Once the BRB cores were designed, the corresponding expected forces in tension and compression were calculated. The selected member sizes of the buildings are summarized in appendix 1. Each gives the selected sections for both BRBF and RL-BRBF with pined and fixed braced-bay beam-to-column connections. Appendix 1 also contains the design

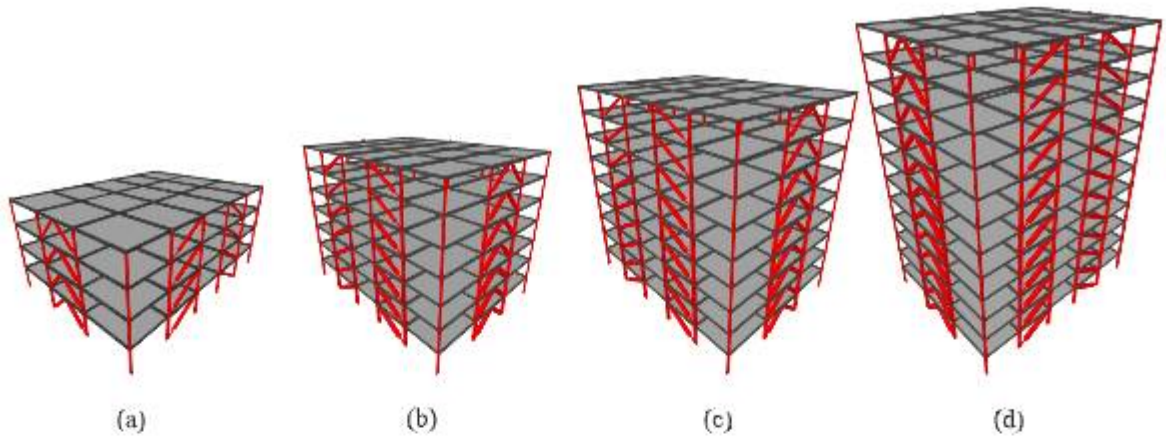

Fig. 3. Three-dimensional overview of the case study buildings (RL-BRBF configuration shown only), (a) 4-story building, (b) 7-story building, (c) 9-story building, (d) 12-story building.

Table 1
Seismic properties of the case study buildings.

Case study building	Fundamental period (per ASCE-7, 16)	Seismic mass (kN)	Design base shear (kN)
4-story	0.53	10938	1400
7-story	0.8	19688	2520
9-story	0.97	25547	3270
12-story	1.2	34231	3560

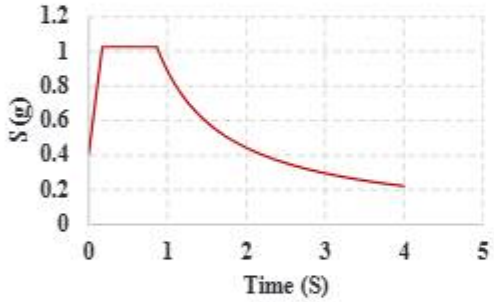

Fig. 4. Design spectrum used for case study structures.

results for the 4-story dual SMRF-BRBF.

4. Structural Analysis

4.1. Finite element modeling

Numerical macro models were formulated to represent the lateral behavior of Buckling Restrained Braced Frames (BRBFs) in both chevron and diagonal configurations within the SeismoSoft SeismoStruct software [25]. These models were constructed employing a combination of elastic beam-column elements and springs to account for lumped plasticity. The BRB cores and elastic pipe sections were respectively characterized using Truss and Non-linear beam-column elements. Additionally, the rotational stiffness of the gusset plates was integrated using a stiffness factor.

To determine the stiffness factor for each beam-column member, a series of Finite Element (FE) analyses were conducted on individual sections with and without gusset plates, considering configurations with one end and both end gussets. The FE analysis results yielded average stiffness factor values of 1.85 and 1.33 for beam-columns with two gussets and one gusset, respectively.

In consideration of the P-Delta effect of the gravity frames, a single leaning column was included in the model. The horizontal translation of the primary nodes at each floor level, including those associated with the leaning column, was constrained using rigid diaphragms. Fig. 6 provides an illustration of the macro modeling approach employed.

The lumped plasticity was incorporated at the beam-to-column connections for rigidly connected beams and for columns. The non-linear moment-curvature of the corresponding sections were adopted to Modified Ibarra-Medina-Krawinkler (MIMK) [26,27] springs as shown in Fig. 7. The MIMK springs can simulate both monotonic and cyclic deterioration of moment capacity. The Interaction of axial force and bending moment at flexural plastic hinges was accounted for by reducing the beam bending moment capacity based on the theory of plasticity. Previous studies have pointed out that conventional BRBs ultimately reach 1 %. This value obviously be higher in RL-BRBs as they are generally shorter in the fuse length. The expected induced can be linearly acquired, meaning that the RL-BRB with 20 % of total length as fuse length will reach a strain demand of 5 %. This value was also confirmed by experiments conducted by Razavi et al., furthermore, their investigations have shown that this strain demand is well within the

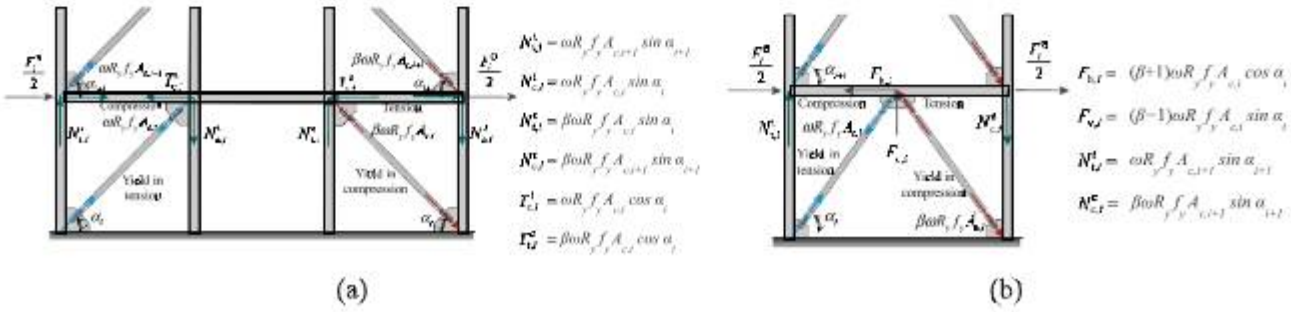

Fig. 5. The expected forces caused by the BRB yielding, (a) diagonal bracing configuration, (b) Chevron bracing configuration.

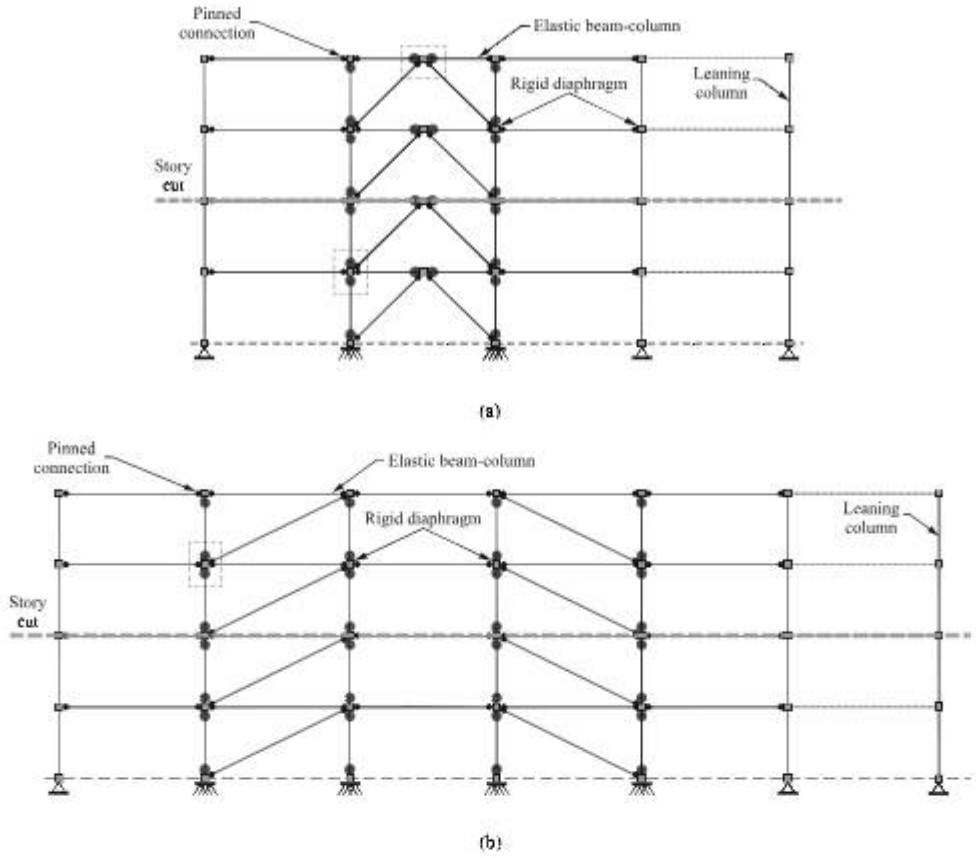

Fig. 6. Two-dimensional finite element macro model of BRBFs in (a) Chevron configuration and (b) Diagonal configuration.

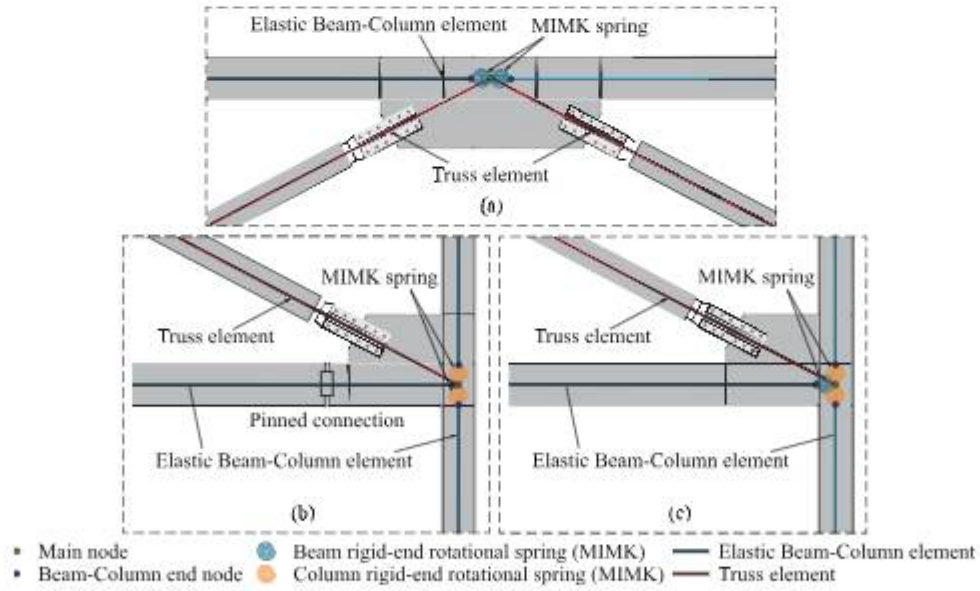

Fig. 7. Connection simulation: (a) Chevron BRBF; (b) Diagonal BRBF with pined beam connection; and (c) Diagonal BRBF with fixed beam connection.

capacity of the RL-BRBs and is not the ultra-low cycle fatigue range. This value was considered as the ultimate strain capacity for the braces.

4.2. Calibration

Giuffre-Menegotto-Pinto (GMP) steel model was used for the BRB and RL-BRB cores. The GMP model can precisely simulate the asymmetrical hysteretic isotropic hardening of the cores. To verify the adopted model, the required parameters were carefully calibrated with experimental results. For this purpose, the hysteretic loops obtained by Eryasar & Topkaya [28] and Razavi et al., [20] were used for BRB and RL-BRB respectively. The adopted parameters can be seen in Table 2. The verified hysteric loops are depicted in Fig. 8 and Fig. 9.

Table 2
Calibrated Giuffre-Menegotto-Pinto (GMP) steel model for BRB and RL-BRB.

Material Properties	Conventional BRB	RL-BRB
Modulus of elasticity (Es)(kPa)	2.00E + 08	262000
Strain hardening parameter (μ)	0.01	0.01
Initial Value of Curvature Parameter (R0)	23	23
Curvature Degradation Parameter (R1)	0.925	0.94
Curvature Degradation Parameter (R2)	0.15	0.14
Isotropic Hardening in Compression Parameter (A2)	2	2
Isotropic Hardening in Tension Parameter (A3)	0.03	0.03
Isotropic Hardening in Tension Parameter (A4)	1	1

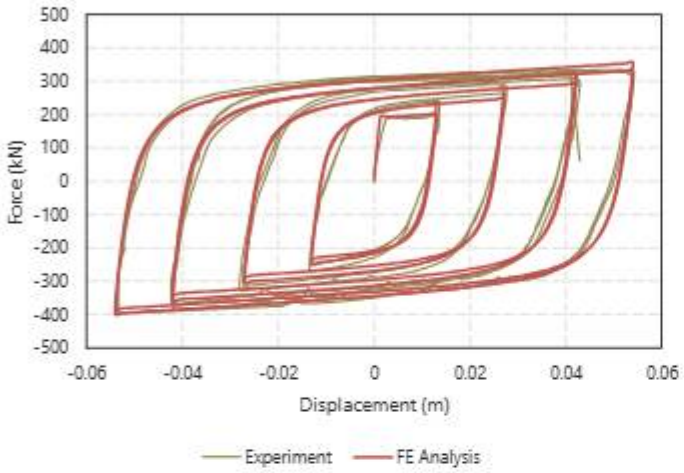

Fig. 8. RL-BRB axial force-axial displacement (experimental data by Razavi et al. [20]).

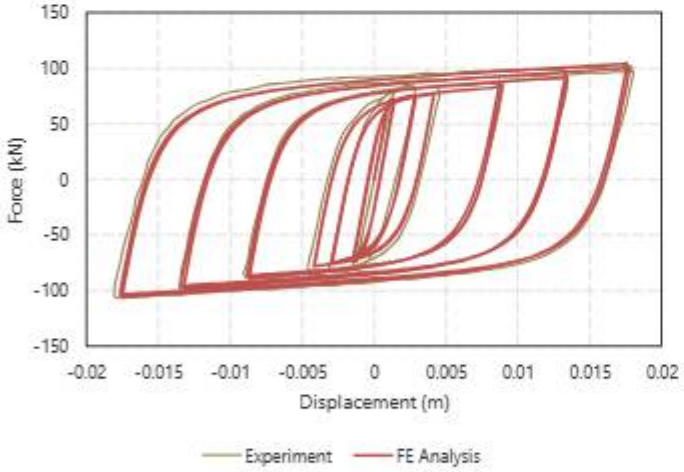

Fig. 9. BRB axial force-axial displacement (experimental data by Eryasar et al., 2009, [28]).

5. Lateral response assessment methods

5.1. Influence of core length on natural period of buckling-restrained braced frames

The buckling-restrained braced frame (BRBF) is a highly effective lateral resisting system that serves as an improved version of conventional concentric braces through the prevention of global buckling. The BRBF system is capable of providing enhanced energy dissipation and higher ultimate capacity owing to its almost symmetric behavior in both tension and compression. Recent studies have demonstrated that reducing the yielding segment of the core can lead to a further improvement in the lateral performance of the BRBF system. Specifically, this reduction results in a significant decrease in the drifts and residual drifts of the structure.

However, this improved lateral performance is accompanied by an increase in the lateral stiffness of the frame, which in turn results in a lower natural period than the expected values in guidelines such as ASCE 7. The accurate prediction of the natural period is essential for the safe design of these structures. Thus, the influence of the core length on the natural period was investigated in this study.

To this end, 49 analyses were conducted on four buildings of varying heights (four, seven, nine, and twelve-story structures) equipped with conventional and reduced core length buckling-restrained braces (RL-BRBs) in both diagonal and chevron configurations. Two core lengths, i.e., 20 % and 40 % of the total brace length, were considered for the RL-BRBs. The study also examined both pinned and rigid braced bay beam-to-column connections.

As a result of this investigation, a new relation was proposed that can predict the natural period of the RL-BRBFs. This relation will be of significant benefit to designers and engineers in ensuring the safety and effectiveness of these structures. Overall, this study underscores the importance of considering the effects of the yielding segment of the core in the design of BRBFs and provides valuable insights into their lateral performance and natural period.

5.2. Influence of core length on natural period of buckling-restrained braced frames

The analytical results show that the braced bay beam connection rigidity decreases the structural period, although this reduction is too little and can be neglected. Furthermore, the diagonally braced frames exhibited higher values of natural period despite possessing two braced bays in total five compared to one braced bay in three bays of inverted chevron braced frames. As anticipated, the core length reduction results in substantial increase in lateral stiffness of the frames which reduces the first mode period of the structure. This decrease in the period can increase the design base shear which is currently neglected in the ASCE 7–16. The code does not account the influence of core length and treats the RL-BRBFs the same as conventional BRBFs. Moreover, the fundamental period per ASCE 7–16 is generally more conservative in taller buildings. This negligence in the increase of lateral stiffness can significantly underestimate the actual structural demand. As a solution, a factor is derived from the comparison of the results which undertakes the influence of core length reduction in natural period of the RL-BRBFs. The proposed factor is as follows:

$$T_a = \alpha C_t h^x \quad \text{(a)}$$

In which, T_a is the fundamental period of the structure, C_t and x are 0.03 and 0.75 for BRBF respectively, and α is the proposed factor calculated as follows:

$$\alpha = 0.77\left(0.3\frac{L_c}{L_b} + 1\right) \quad \text{(b)}$$

In which, L_c is the core length, L_b is the total brace length.

5.3. Push-over FEA and lateral collapse parameters

Nonlinear static analysis, commonly known as Pushover analysis, offers a comprehensive insight into the lateral performance of Buckling Restrained Braces (BRBs). This method enables us to examine the impact of the yielding segment of the core and the contribution of braced bay frame action. To achieve this, a case study was conducted, where structures were analyzed under two different lateral load patterns. The first pattern was mass proportionate at each story level, while the second

pattern was equivalent to the structural deformed shape in the first mode shape. The most critical scenario among the two was selected as the structural lateral response. Additionally, a novel direct method is proposed in this study to determine the structural response modification factor of the structures. This technique is a combination of the Federal Emergency Management Agency's (FEMA) P695 and Uang's method [29,30]. The associated parameters are depicted in Fig. 10.

Nonlinear static analysis, also referred to as Pushover analysis, provides an in-depth understanding of the lateral performance of Buckling Restrained Braces (BRBs). This analytical method allows for the evaluation of the yielding behavior of the core segment and the contribution from the braced bay frame action. To investigate this, a case study was conducted involving structural analysis under two distinct lateral load patterns: one proportional to the mass at each story level, and the other corresponding to the structure's deformed shape in its first mode. The more critical of the two scenarios was identified as the primary structural lateral response.

Furthermore, this study introduces an innovative direct method for determining the structural response modification factor. This method synthesizes elements from the Federal Emergency Management Agency's (FEMA) P695 guidelines and Uang's methodology. The parameters used in this approach are illustrated in Fig. 10. FEMA P695 involves a 20 % reduction in base shear to compute the overstrength and ultimate drift displacement of the structure, providing a realistic and directly calculable estimate. However, it recommends a predictive relationship for calculating the effective yield displacement. Conversely, Uang's method offers a predictive relationship for ultimate drift displacement but overlooks the reduction in base shear, potentially compromising the accuracy of both the overstrength factor (Ω) and the ductility reduction factor (Rμ). Uang's method does consider the equivalent elastic response of the structure, which can be directly derived from the pushover curve.

The advantages of both methods were integrated into a direct lateral response calculation method, referred to as the Direct Method. This method incorporates parameters such as overstrength (Ω), the force reduction factor (Rμ), and the response modification factor (R), which can be derived using relations 1–4 respectively. The overstrength factor (Ω) is quantified as the ratio of the maximum base shear (Vmax) to the first significant yield base shear (Vs) of the structure.

The quantified overstrength (Ω) factor is the ratio of the maximum base shear (V_{max}) to the first significant yield of the structure (V_s):

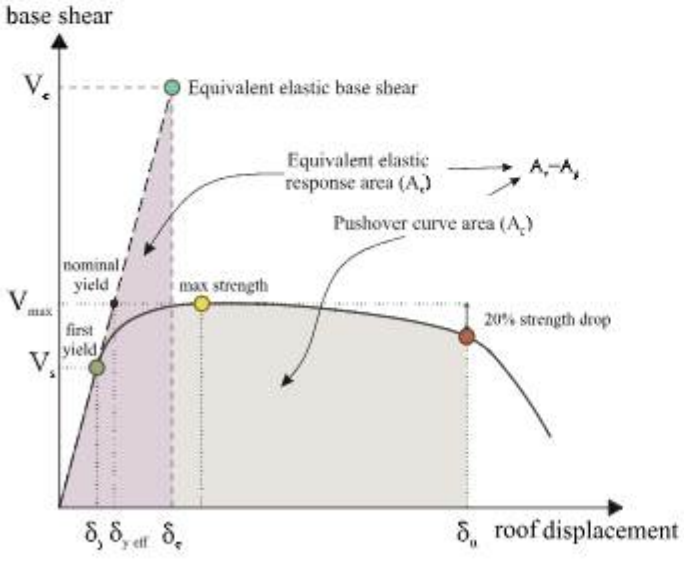

Fig. 10. The pushover curve and associated definitions according to the proposed direct method (combination of FEMA P695 and Uang's method [30]).

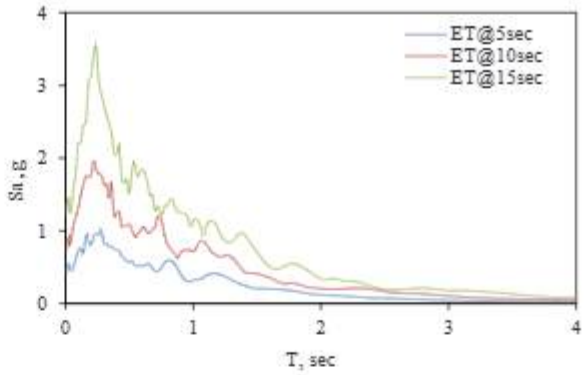

Fig. 11. Linear relationship of spectrum intensity and ET time.

$$\Omega = \frac{V_{max}}{V_s} \tag{1}$$

The force reduction factor is the ratio of the equivalent elastic base shear (V_e) to the first significant yield of the structure (V_s):

$$R_\mu = \frac{V_e}{V_{max}} \tag{2}$$

The response modification factor is the multiplication of overstrength (Ω) factor and The force reduction factor (R_μ):

$$R = \Omega \times R_\mu \tag{3}$$

5.4. Endurance Time Method (ETM) and lateral collapse parameters

To identify the Engineering Demand Parameter (EDP) of a building for a specific seismic event with a defined Intensity Measure (IM), an Incremental Dynamic Analysis (IDA) is essential. However, this analysis can be excessively time-consuming, particularly for complex structures such as the one examined in this study, which renders it impractical. To address this challenge, an inventive dynamic pushover technique called

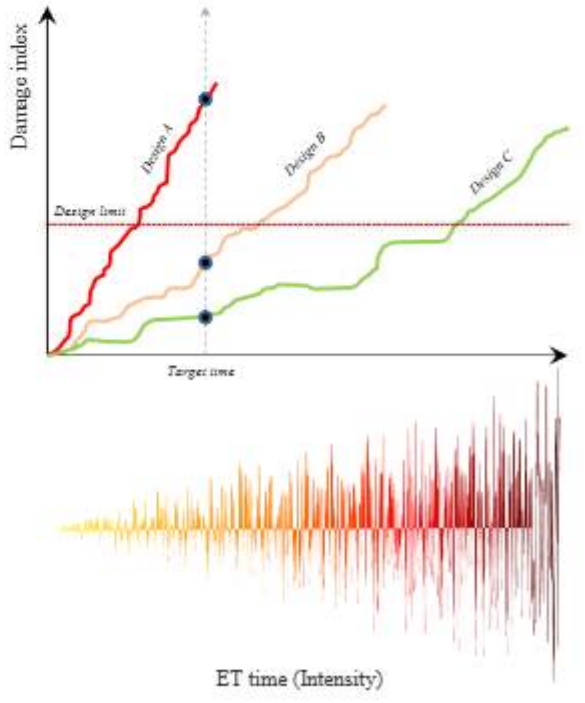

Fig. 12. Schematic representation of ET records and EDP in different design levels.

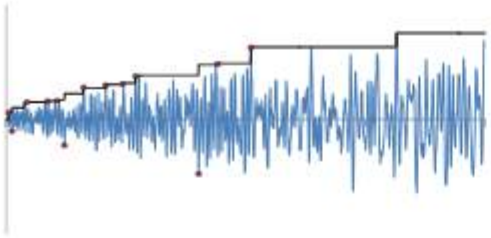

Fig. 13. Method of plotting increasing curves of ET results.

Endurance Time (ET), proposed by Estekanchi et al. [22] is utilized. The ET method is an innovative and efficient method which can replace IDA analysis method with much less analytical time consumption [31–36]. The method has proven to be precise ins a variety of engineering incorporation such as structural design of new buildings, seismic retrofit, and performance design of structures [31–36]. The method has also been verified in different structural systems such as SMRF, CBF, BRBFs [31–36]. These intensifying acceleration functions have been produced making use of numerical and optimization techniques. The main advantage of ET records is that their response spectrum at any time is linearly proportional to the response spectrum at a target time (t_{target} = 8sec) which is summarized in Relation 4–7 and presented in Fig. 11. So, the time in these records is a critical factor determining the intensity of the excitation; the more a typical structure withstands ET records, the more favorable is its seismic performance. This is schematically shown in Fig. 12 which indicated Design A cannot meet codes requirements because the building experiences collapse before reaching the target time. Also, as can be seen in Fig. 13, up to a specific time, the maximum value of each EDP is critical, time-history of the maximum of absolute results of ET records are plotted besides the maximum EDP from real earthquakes.

$$S_{aR}(T,t) = \frac{t}{t_{Target}} S_{aR}(T) \tag{4}$$

$$S_{uR}(T,t) = \frac{t}{t_{Target}} S_{aR}(T) \times \frac{T^2}{4\pi^2} \tag{5}$$

$$CAV_R(T,t) = \frac{t}{t_{Target}} CAV_R(T) \tag{6}$$

$$\begin{aligned} Minimize F(a_\xi) = \int_0^{T_{max}} \int_0^{t_{max}} \Big\{ & |S_a(T,t) - S_{aT}(T,t)|^2 \\ & + \alpha |S_a(T,t) - S_{aT}(T,t)|^2 \\ & + \beta |CAV(T,t) - CAV_T(T,t)|^2 \Big\} dt dT \end{aligned} \tag{7}$$

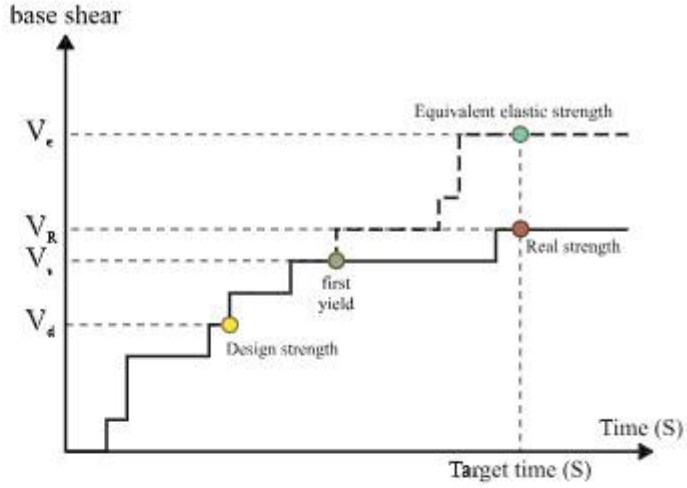

Fig. 15. The processed base shear versus time (intensity) in endurance time method (ETM) [22].

Each of the structures are analyzed under three ETM records as displayed in Fig. 14. It should be noted that the analyses of the structures are carried out both conventionally and once done considering all materials as elastic to acquire the equivalent elastic response of the structures, in other words, each structure was analyzed six times. Subsequently, the base shear versus time (seismic intensity) will be derived and processed according to Fig. 13, thereafter, the structural response parameters are then calculated and illustrated. The structural response parameters were calculated according to Fig. 15 and the same relations used for push-over analyses (relations 1–3), however, in ETM the maximum base shear (V_{max}) is replaced with the real strength of the structure (V_R) at a specific time (intensity). Hence, the relations 8–10 were used for calculating the response parameters. Such method was also used by Mohsenian et al.l., [37]. The findings of their study demonstrate the effectiveness of the Endurance-Time approach in accurately determining the performance level, maximum inter-story drift distribution, and structural responses of steel moment-resisting frames, while incurring lower computational expenses in comparison to traditional techniques [37].

The quantified overstrength (Ω) factor is defined as the ratio of the structural real strength (V_R) to the first significant yield of the structure (V_s):

$$\Omega = \frac{V_R}{V_s} \tag{8}$$

The force reduction factor is now defined as the ratio of the

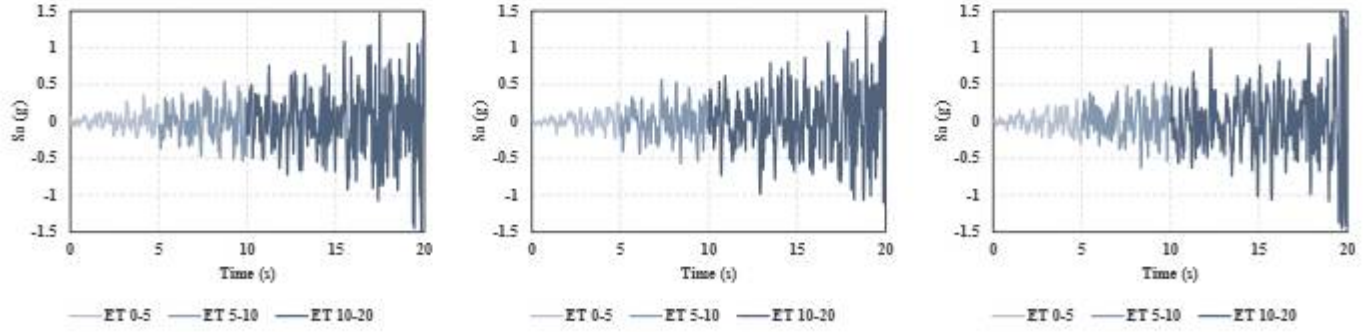

ETA20inx01 ETA20inx02 ETA20inx03

Fig. 14. The ETA records used for FEA of structures [22].

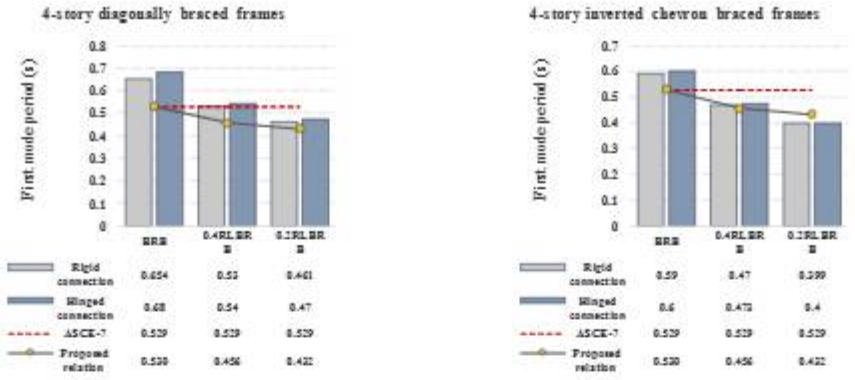

The comparison of the analyctical and ASCE 7-16 values of natural period for 4-story frames.

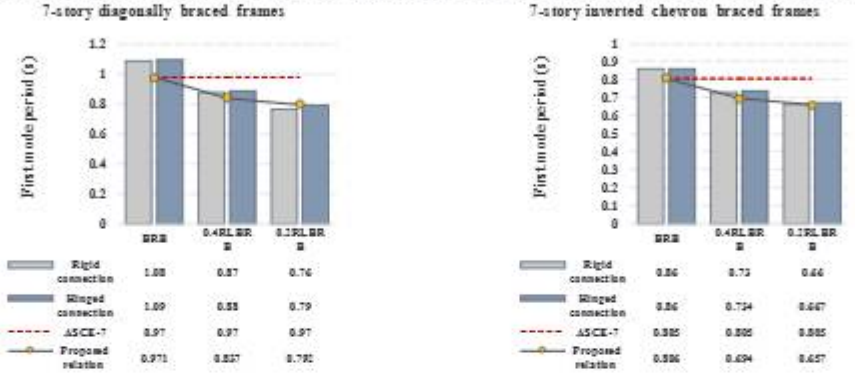

The comparison of the analyctical and ASCE 7-16 values of natural period for 7-story frames.

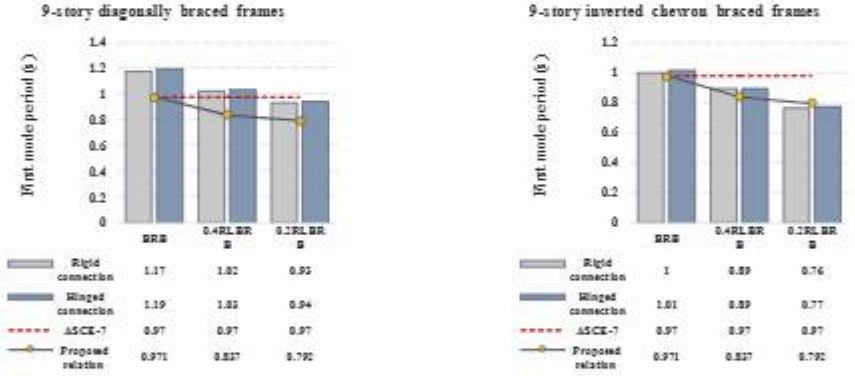

The comparison of the analyctical and ASCE 7-16 values of natural period for 9-story frames.

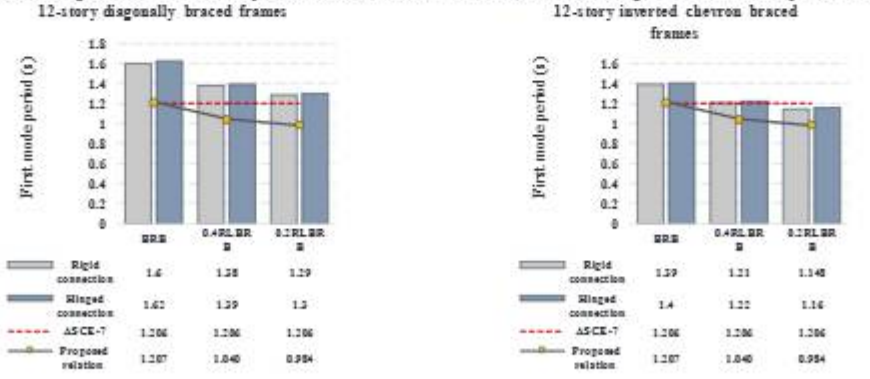

The comparison of the analyctical and ASCE 7-16 values of natural period for 12-story frames.

Fig. 16. The comparison of the analyctical and ASCE 7–16 values of natural period for case study buildings.

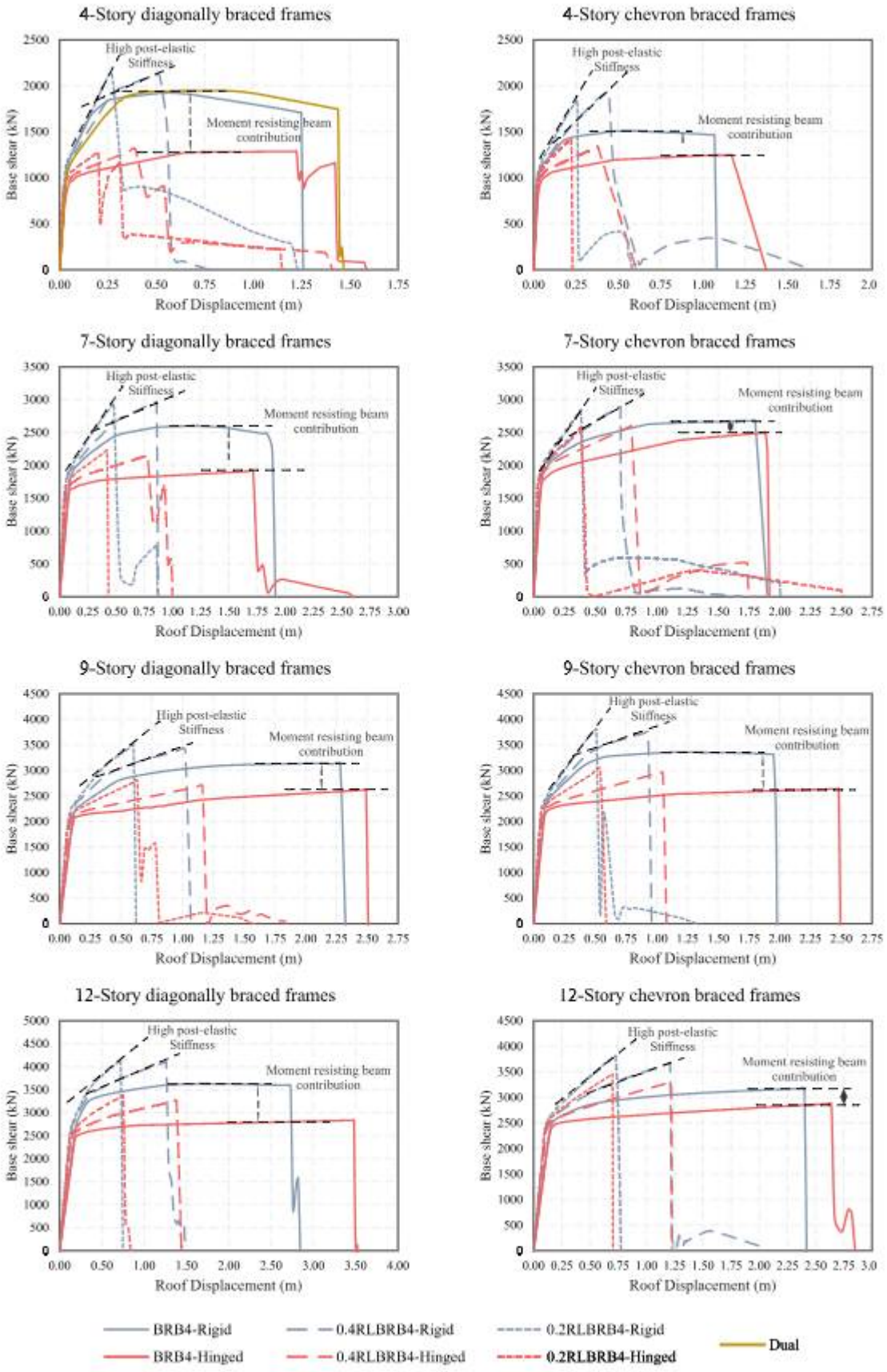

Fig. 17. The pushover FEA results.

Table 3
Seismic response parameters of the case study structures.

Seismic response parameters of the 4-story diagonally braced frames												
	V_s (kN)		V_{max} (kN)		V_e (kN)		Ω		R_μ		R	
	hinged	fixed	hinged	fixed	hinged	fixed	hinged	fixed	hinged	fixed	hinged	fixed
Dual	–	1164.93	–	1948.55	–	9954.43	–	1.67	–	8.55	–	14.29
Conv BRB	942.87	1104.18	1286.49	1924.83	7358.89	10223.70	1.36	1.74	7.80	9.26	10.65	16.14
0.4 BRB	939.78	1146.46	1311.80	2124.05	4227.46	6857.33	1.40	1.85	4.50	5.97	6.28	11.04
0.2 BRB	974.02	1187.29	1278.46	2133.07	3729.42	5515.77	1.31	1.80	3.83	4.65	5.03	8.35
Seismic response parameters of the 4-story Inverted V braced frames												
Conv BRB	960.82	1020.30	1245.40	1510.77	7616.73	9664.36	1.30	1.48	7.93	9.47	10.28	14.03
0.4 BRB	1005.50	1052.80	1337.79	1936.96	4690.25	6665.28	1.33	1.84	4.65	6.33	6.19	11.65
0.2 BRB	1014.92	1073.52	1423.88	1846.97	4225.30	6092.56	1.40	1.72	4.16	5.68	5.84	9.76
Seismic response parameters of the 7-story diagonally braced frames												
Conv BRB	1602.45	1629.84	1913.36	2602.25	11345.34	13781.02	1.19	1.60	7.08	8.46	8.45	13.50
0.4 BRB	1634.81	1715.88	2148.09	2962.45	8807.20	10898.80	1.31	1.73	5.39	6.35	7.08	10.97
0.2 BRB	1686.97	1801.99	2224.82	2939.28	6621.96	8064.93	1.32	1.63	3.93	4.48	5.18	7.30
Seismic response parameters of the 7-story Inverted V braced frames												
Conv BRB	1780.72	1859.88	2224.82	2681.17	13394.98	14816.20	1.25	1.44	7.52	7.97	9.40	11.48
0.4 BRB	1867.50	1863.75	2599.02	2867.29	9287.46	10284.04	1.39	1.55	4.97	5.52	6.92	8.55
0.2 BRB	1872.82	1912.74	2569.31	2845.04	7208.06	7746.43	1.37	1.49	3.85	4.05	5.28	6.02
Seismic response parameters of the 9-story diagonally braced frames												
Conv BRB	1872.82	2178.30	2612.55	3139.12	12804.90	15420.50	1.39	1.44	6.84	7.08	9.54	10.20
0.4 BRB	2143.88	2295.09	2698.70	3409.02	9084.73	10515.48	1.26	1.49	4.24	4.58	5.33	6.81
0.2 BRB	2161.83	2295.31	2801.35	3484.77	7744.19	8435.50	1.30	1.52	3.58	3.68	4.64	5.58
Seismic response parameters of the 9-story Inverted V braced frames												
Conv BRB	2205.69	2319.47	2635.72	3356.04	15636.43	16808.77	1.19	1.45	7.09	7.25	8.47	10.49
0.4 BRB	2232.47	2478.71	2950.00	3750.04	11575.86	12597.61	1.32	1.51	5.19	5.08	6.85	7.69
0.2 BRB	2261.95	2419.66	3029.71	3799.22	8201.24	8872.76	1.34	1.57	3.63	3.67	4.86	5.76
Seismic response parameters of the 12-story diagonally braced frames												
Conv BRB	2507.22	2585.99	2835.12	3628.39	14893.90	16276.18	1.13	1.40	5.94	6.29	6.72	8.83
0.4 BRB	2562.93	2613.06	3260.46	4103.81	10942.01	12854.39	1.27	1.57	4.27	4.92	5.43	7.73
0.2 BRB	2565.58	2649.66	3372.34	4139.02	8518.47	9484.56	1.31	1.56	3.32	3.58	4.36	5.59
Seismic response parameters of the 12-story Inverted V braced frames												
Conv BRB	2448.06	2479.06	2875.45	3174.76	13723.84	14451.13	1.17	1.28	5.61	5.83	6.58	7.47
0.4 BRB	2507.47	2522.87	3300.35	3667.63	10630.23	11662.51	1.32	1.45	4.24	4.62	5.58	6.72
0.2 BRB	2533.18	2554.96	3458.79	3813.42	8658.94	9494.75	1.37	1.49	3.42	3.72	4.67	5.55

equivalent elastic base shear (V_e) to the structural real strength (V_R):

$$R_\mu = \frac{V_e}{V_R} \tag{9}$$

The response modification factor is unchanged and defined as the multiplication of overstrength (Ω) factor and The force reduction factor (R_μ):

$$R = \Omega \times R_\mu \tag{10}$$

lateral Response Assessment results

FEA results are presented in this section. It should be reminded that single frames were modeled in the FE software, representing one of the existing two structural lateral resisting frames in the whole structure and consequently exhibiting half of the overall shear capacity. Hence, the shear capacities should be doubled when compared with design values presented in Table 1. The aforementioned obviously does not influence the obtained response parameters in any way whatsoever.

5.5. Influence of core length on natural period of buckling-restrained braced frames

As depicted in Fig. 16, The proposed factor can adequately predict the core length effect while marinating the conservativity in taller structures, as intended in the ASCE 7–16. It is recommended herein to use the proposed relation when one is going to design the structure with RL-BRBF as the main lateral resisting system.

Prediction of natural period of the structures is the first step to seismic design of structures. The current ASCE 7–16 relation does not consider the influence of core length reduction the natural period of the RL-BRBFs. To assess the aforementioned effect, 48 frames are analyzed and compared. The results are:

A factor (α) is derived from the numerical results which adds the core length influence to the current ASCE 7–16 relation. The proposed relation shows great accuracy in predicting the natural period of the low to mid-rise structures and is conservative in high-rise buildings, as is the ASCE 7–16. It was also noted that the braced bay beam connection has insignificant influence on the structural period. The diagonally braced frames possess lower values of natural period even though they have higher redundancy.

5.6. Push-over FEA results

The pushover analysis results are illustrated in Fig. 17. As can be seen, the moment resisting beams contributed to the overstrength factor of the frames. The 4-story dual frame performed almost the same as the moment resisting frame. Furthermore, reducing the core length of the BRBs resulted in an increase in the post-elastic stiffness of the frames which also resulted in higher ultimate shear force capacity. Additionally, the BRBFs with hinged braced bay beams exhibited the least overstrength compared to the rest of the frames. The fatigue appeared to be the governing factor in limiting the ultimate displacement capacity of the frames. The RL-BRBs ruptured in lower drift amplitudes due to the core length reduction and the fatigue, hence, the ductility has drastically decreased. Though less drift capacity is observed in the RL-BRBFs, the earthquake induced drifts are expected to decrease due to the higher stiffness. More quantitative results are given in Table 3. Overall, the results show an increase in overstrength by fixing the braced bay beam connection which led to increase the (Ω) factor from an average value of approximately 1.2 to an average value of 1.45 for conventional BRB. This increase was calculated to be 1.33 1.62 for 0.4 core length RL-BRBFs and 1.34–1.63 in the 0.2 core length RL-BRBFs. In contrast to overstrength, the reduction in core length resulted in a decrease in the ductility factors which was expected. However, the fixed connection of the braced bay beams compensated for this disadvantage to some

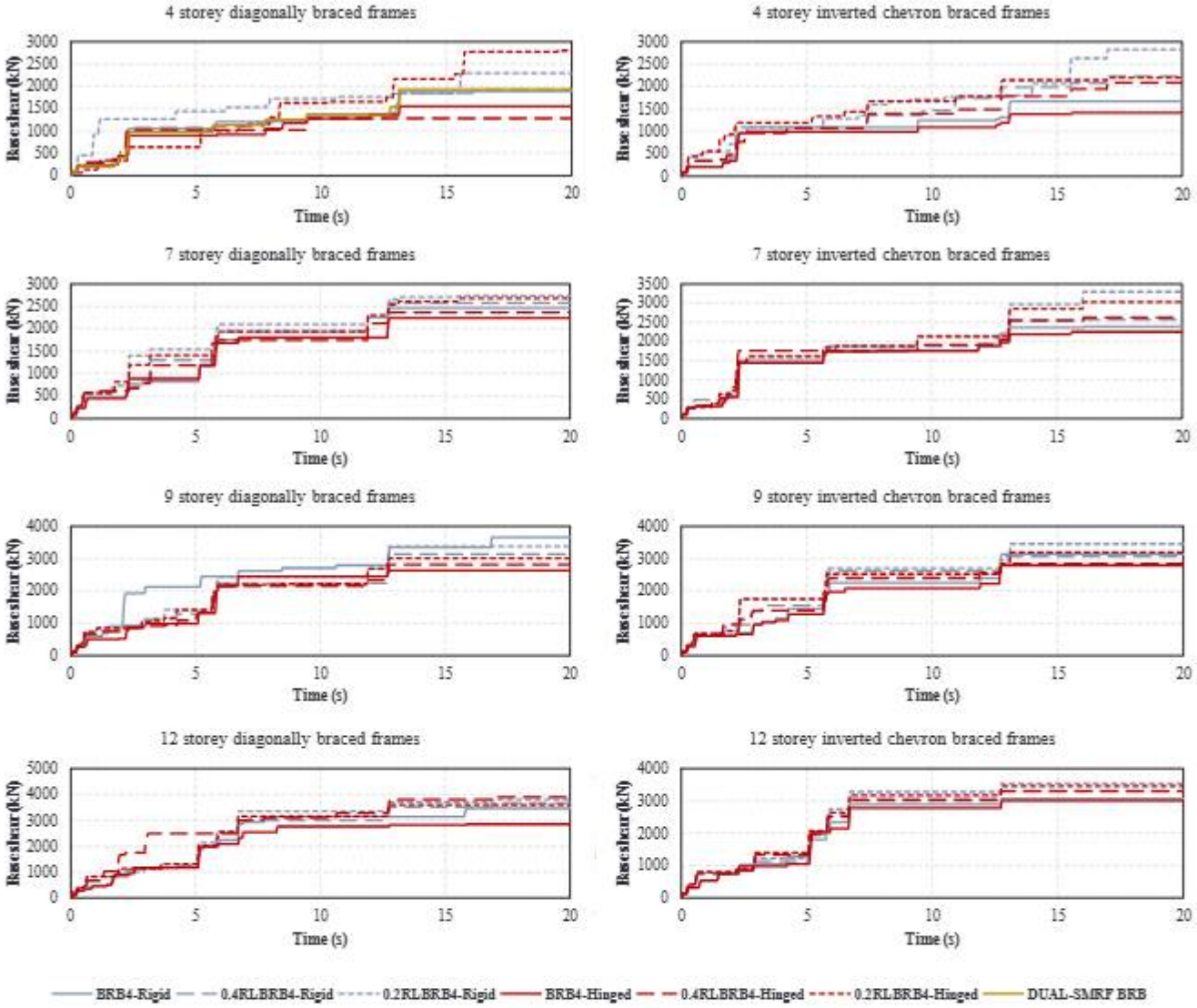

Fig. 18. ETM base shear versus time (intensity).

degree. The (μ) factor of the 0.2 core length RL-BRBFs were evaluated as least, which were calculated as to an average of approximately equal to 3.71 in the hinged braced beams and 4.27 in the fixed braced beams. The derived response modification factors were equal to 4.98, 6.21, 8.76 in the 20 %, 40 %, and 100 % (conventional BRB) of the core length BRBFs with hinged braced bay beams and 7.03, 8.89, 11.07 in the fixed braced bay beams, correspondingly. It should be noted that the results indicate the ultimate lateral response capacity of the structures without considering the demand and real-life performance of the structures. As evident, the push-over curves have all ended at an unstable stage indicating lateral collapse, which was caused by the predefined ultimate strain of 5 % considered for the BRB cores. This strain rate was the highest expected strain exhibition reported by several previously conducted experimental research [20,38–40]. This decrease in the response modification factors do not necessarily mean degradation in performance level of the RL-BRBFs, especially since such high levels of drifts (the ultimate capacities derived in conventional BRBFs) are not probable in structures, hence the conventional BRBs ductility (μ), ductility reduction factor (R_μ), and response modification factors (R) will be below the calculated ultimate values. In contrast, in the case of the RL-BRBs, these values are at levels which are expected to occur during a seismic event. Ergo, it is an indication that the structures can withstand the expected lateral forces with the same cost while maintaining higher levels of elasticity by providing post-elastic stiffness and decreasing the lateral drift demand in conjugation to an increase in lateral force capacity demand. Hence, nonlinear dynamic analyses must be performed to assess the real-time performance of the structures and assess the response parameters while fully considering the seismic demand of each structure.

5.7. Endurance Time Method (ETM) FEA results

The ETM analyses results are presented in this section. The total base shear versus seismic intensity (time) of the case structures are depicted in Fig. 18. As can be seen, it is evident that decreasing the core length of the BRBs have resulted in an increase in the induced base shear, in other words, an increase in the lateral force demand. This increase in demand is significantly less apparent in taller structures. The derived response parameters according to ETM method previously explained in Fig. 13 and relations (8) to (10) are illustrated versus seismic intensity (ETM record time in S) in Fig. 19. The quantified values of the parameters are reported in Table 4 for two seismic levels, namely, DBE earthquake with exceedance probability of 10 % in 50 years (475-year return period) MCE earthquake with exceedance probability of 2 % in 50 years (2475-year return period). The overstrength factors (Ω) at the DBE level were calculated as equal to an average of 1.14, 1.16, and 1.28 in the BRBFs

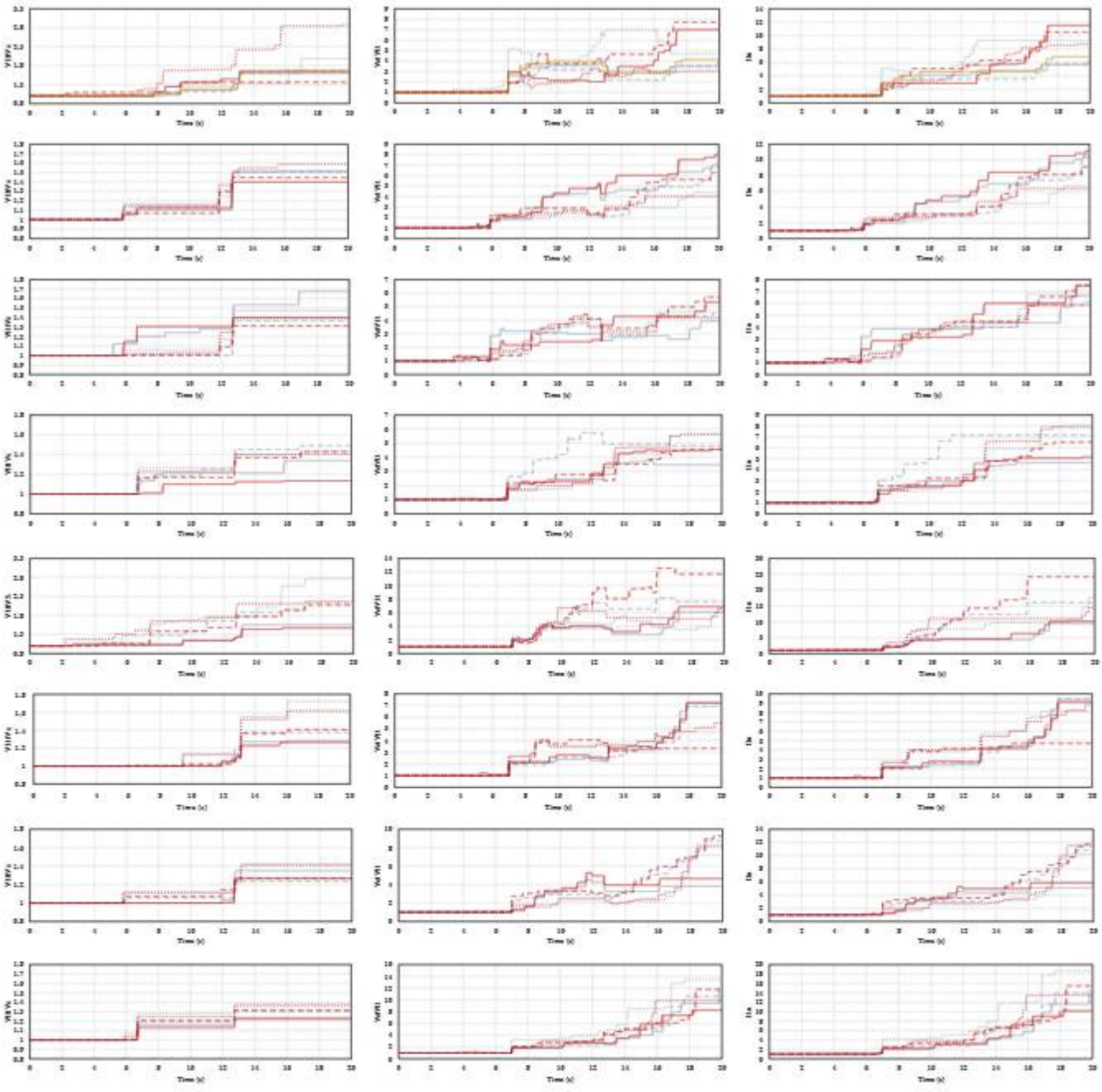

Fig. 19. ETM structural response parameters versus time (intensity).

with hinged braced baby beams and 1.13, 1.14, and 1.24 in BRBFs with fixed braced baby beams for the conventional BRBFs, RL-BRBFs with 0.4 core length, and RL-BRBFs with 0.2 core length, respectively. The values were calculated 1.34, 1.40, and 1.73 for hinged braced bay beams and 1.41, 1.47, 1.71 in the brace bay beams with fixed connections in the MCE level, correspondingly. The average value of ductility reduction factor increased from 2.87 in hinged bay beam BRBF to 3.27 in fixed braced bay beam in the RL-BRBF with 0.2 of core length as the yielding segment, in the DBE level of seismicity. Consequently, at MCE level, the ductility reduction factor increased from an average of 3.41 In the conventional BRBFs to 4,55 in the RL-BRBFs with 0.2 core length. Ultimately, the average values for the seismic response modification factors also increased in RL-BRBFs, much expectedly, see Table 5. The results indicate close performance in RL-BRBs with 40 % and 20 % core lengths, hence, 40 % of total brace length as the yielding segment of the BRB can be the optimum core length, since as the core length decreases so does the ultimate drift capacity. The 9-story structure shows a notable improved response in the inverted chevron braced configuration compared to the diagonally braced system. The 7-story structures appear to have performed similarly up to 13.5 seconds (approximately) in the inverted chevron braced frame, while the RL-BRBFs exhibited increased base shear capacity in the diagonally braced frames. This shows frequency sensitivity in the system. Over all the results show that the diagonally braced RL-BRBFs possess increased base shear capacities.

5.8. Concluding remarks

Lateral response of Buckling-Restrained Braced Frames (BRBFs) was evaluated while considering principal factors such as yielding core length variety in the BRBs, rigidity and moment capacity of the braced

Table 4
Seismic response parameters of the case study structures according to ETM.

	DBE earthquake with exceedance probability of 10 % in 50 years (475-year return period)						MCE earthquake with exceedance probability of 2 % in 50 years (2475-year return period)					
Seismic response parameters of the 4-story diagonally braced frames												
	Ω		R_μ		R		Ω		R_μ		R	
	hinged	fixed	hinged	fixed	hinged	fixed	hinged	fixed	hinged	fixed	hinged	fixed
Dual	–	1.17	–	3.98	–	4.66	–	1.66	–	2.81	–	4.66
Conv BRB	1.36	1.16	2.16	3.56	2.93	4.13	1.65	1.59	3.49	3.02	5.75	4.79
0.4 BRB	1.36	1.11	3.75	3.19	5.12	3.55	1.36	1.61	4.65	2.21	6.34	3.55
0.2 BRB	1.67	1.25	1.96	3.67	3.27	4.58	2.87	1.99	3.26	6.98	9.35	13.86
Seismic response parameters of the 4-story Inverted V braced frames												
Conv BRB	1.13	1.16	3.77	3.75	4.28	4.34	1.44	1.55	4.38	2.79	6.30	4.34
0.4 BRB	1.39	1.39	4.39	3.87	6.08	5.36	1.77	1.89	9.55	6.57	16.94	12.38
0.2 BRB	1.65	1.68	6.70	4.61	11.05	7.75	2.16	2.76	5.24	4.81	11.34	13.29
Seismic response parameters of the 7 story diagonally braced frames												
Conv BRB	1.13	1.10	4.33	4.19	4.68	4.62	1.40	1.51	6.02	4.63	8.42	6.99
0.4 BRB	1.07	1.13	2.91	2.55	3.11	2.89	1.45	1.50	4.57	3.57	6.61	5.36
0.2 BRB	1.15	1.17	2.40	2.21	2.75	2.57	1.59	1.52	3.38	2.97	5.37	4.51
Seismic response parameters of the 7-story Inverted V braced frames												
Conv BRB	1.00	1.00	2.76	2.38	2.76	2.38	1.23	1.27	3.49	3.19	4.29	4.07
0.4 BRB	1.02	1.01	3.73	2.56	3.63	2.59	1.36	1.38	3.44	3.22	4.69	4.43
0.2 BRB	1.14	1.12	3.54	3.38	4.02	3.79	1.62	1.72	3.95	3.88	6.38	6.68
Seismic response parameters of the 9-story diagonally braced frames												
Conv BRB	1.31	1.24	2.42	3.10	3.16	3.85	1.40	1.53	4.29	2.83	6.01	4.34
0.4 BRB	1.01	1.00	3.38	3.05	3.40	3.05	1.31	1.37	3.41	2.93	4.48	4.00
0.2 BRB	1.02	1.06	3.74	3.53	3.83	3.73	1.39	1.47	3.17	2.70	4.41	3.98
Seismic response parameters of the 9-story Inverted V braced frames												
Conv BRB	1.00	1.00	3.32	3.05	3.32	3.05	1.27	1.35	3.94	3.26	4.98	4.40
0.4 BRB	1.07	1.05	3.30	2.94	3.55	3.10	1.27	1.24	4.50	4.73	5.72	5.84
0.2 BRB	1.12	1.11	2.52	3.53	2.81	3.92	1.41	1.43	2.44	2.24	3.44	3.19
Seismic response parameters of the 12-story diagonally braced frames												
Conv BRB	1.10	1.21	2.30	2.45	2.53	2.97	1.12	1.21	4.40	3.68	4.94	4.47
0.4 BRB	1.17	1.19	2.78	4.20	3.24	4.98	1.37	1.45	3.52	4.94	4.81	7.17
0.2 BRB	1.23	1.26	1.98	1.78	2.43	2.25	1.40	1.44	4.71	4.26	6.60	6.12
Seismic response parameters of the 12-story Inverted V braced frames												
Conv BRB	1.10	1.16	1.93	2.02	2.12	2.35	1.22	1.24	5.93	3.91	7.25	4.84
0.4 BRB	1.17	1.21	2.74	2.30	3.20	2.79	1.31	1.31	5.04	5.08	6.62	6.66
0.2 BRB	1.23	1.28	3.05	3.45	3.75	4.42	1.36	1.38	4.84	8.52	6.61	11.80

Table 5
ETM average seismic response parameters for DBE and MCE seismic levels.

	DBE earthquake with exceedance probability of 10 % in 50 years (475-year return period)						MCE earthquake with exceedance probability of 2 % in 50 years (2475-year return period)					
	Ω		**R_μ**		**R**		**Ω**		**R_μ**		**R**	
	hinged	**fixed**	**hinged**	**fixed**	**hinged**	**fixed**	**hinged**	**fixed**	**hinged**	**fixed**	**hinged**	**fixed**
Conv BRB	1.14	1.13	2.67	3.06	3.25	3.46	1.34	1.41	4.49	3.41	5.99	4.78
0.4 BRB	1.16	1.14	3.37	3.08	3.94	3.54	1.40	1.47	4.83	4.15	7.03	6.17
0.2 BRB	1.28	1.24	3.24	3.27	4.24	4.13	1.73	1.71	3.87	4.55	6.69	7.93

bay beams, structural height, and bracing configuration. A total of 49 structures were designed and subsequently analyzed under static and dynamic loadings. Endurance Time Method (ETM) were used for nonlinear time history analyses (NLTHs) to reduce the excessive number of analyses. Seismic response parameters were then derived from each FEA and the noteworthy results are presented as follows:

- A novel relationship was proposed to predict the fundamental period of RL-BRB structures. This approach accurately estimated the natural period for low to mid-rise buildings but was conservative for high-rise structures, aligning with ASCE 7–16 standards. The study found that the connection of the braced bay beam had minimal impact on structural period. Interestingly, diagonally braced frames exhibited lower natural periods despite higher redundancy.
- Reducing yielding segments in RL-BRBs significantly boosted post-elastic stiffness, reducing seismically induced drifts according to nonlinear static analyses (push-over).
- Both the 4-story dual SMRF-BRBF and BRBF showed comparable performance in static and dynamic analyses.
- Push-over results indicated an increase in overstrength factor (Ω) for conventional BRBs, rising from approximately 1.2 to 1.45. For 0.4 core length RL-BRBFs, Ω increased from 1.33 to 1.62, and for 0.2 core length RL-BRBFs, from 1.34 to 1.63.
- Response modification factors derived from push-over analyses increased with shorter core lengths, ranging from 4.98 to 8.76 for hinged braced bay beams and from 7.03 to 11.07 for fixed braced bay beams.
- ETM analyses showed a similar trend in increasing overstrength factor (Ω) for reduced core length BRBs but revealed that ultimate ductility of conventional BRBs exceeded structural demand. Consequently, ductility reduction factors increased as core length decreased.
- Response modification factors (R) from ETM analyses increased for RL-BRBs, ranging from approximately 3.25 to 4.24 in DBE level and from 4.78 to 7.93 in MCE level, with 20 % core length yielding optimal results for drift capacities.

A multi-level seismic performance assessment considering several influencing factors such as braced bay connection, yielding segment fore

length, ultimate state capacities, and Endurance Time Method (ETM) were considered in this investigation to embark on less investigated aspects of the BRBF system. Though several aspects of the proposed system were scrutinized, further research is needed to continue the advancement of knowledge in the much popular BRBF systems.

Appendix

Appendix 1 Structural design results (AISC section library.)

Selected members for 4-story Chevron BRBF.

Story	Braced bay column	Braced bay Beam	BRB Core Area (mm^2)	Elastic Pipe (RL-BRB only)
4	W14X53	W12X35	968	PIPE10X0.625
3	W14X53	W12X35	2258	PIPE14X0.625
2	W14X53	W16X36	2581	PIPE16X0.625
1	W14X68	W16X36	2580	PIPE16X0.625

Selected members for 4-story Diagonal BRBF.

Story	Braced bay column	Braced bay Beam	BRB Core Area (mm^2)	Elastic Pipe (RL-BRB only)
4	W14X53	W12X35	645	PIPE10X0.375
3	W14X53	W12X35	1613	PIPE14X0.500
2	W14X53	W16X36	2258	PIPE14X0.625
1	W14X68	W16X36	2258	PIPE14X0.625

Selected members for 4-story dual SMRF-BRB frame.

Story	Braced bay column	Braced bay Beam	BRB Core Area (mm^2)	SMRF bay column	Elastic Pipe (RL-BRB only)
4	W14X53	W12X35	645	W14X53	PIPE10X0.375
3	W14X53	W12X35	1613	W14X53	PIPE14X0.500
2	W14X53	W16X36	2258	W14X53	PIPE14X0.625
1	W14X68	W16X36	2258	W14X68	PIPE14X0.625

Selected members for 7-story Chevron BRBF.

Story	Braced bay column	Braced bay Beam	BRB Core Area (mm^2)	Elastic Pipe (RL-BRB only)
7	W14X48	W16X26	1290	PIPE14X0.375
6	W14X48	W16X26	2258	PIPE16X0.500
5	W14X61	W16X26	3548	PIPE20X0.625
4	W14X109	W16X36	4194	PIPE20X0.625
3	W14X109	W16X36	4194	PIPE20X0.625
2	W14X211	W16X36	4516	PIPE20X0.625
1	W14X211	W16X36	4516	PIPE20X0.625

Selected members for 7-story Diagonal BRBF.

Story	Braced bay column	Braced bay Beam	BRB Core Area (mm^2)	Elastic Pipe (RL-BRB only)
7	W14X48	W16X26	968	PIPE14X0.375
6	W14X48	W16X26	1613	PIPE16X0.500
5	W14X61	W16X26	2258	PIPE16X0.500
4	W14X61	W16X36	3226	PIPE20X0.625
3	W14X120	W16X36	3871	PIPE20X0.625
2	W14X120	W16X36	3871	PIPE20X0.625
1	W14X120	W16X36	3871	PIPE20X0.625

Selected members for 9-story Chevron BRBF.

Story	Braced bay column	Braced bay Beam	BRB Core Area (mm^2)	Elastic Pipe (RL-BRB only)
9	W14X38	W16X57	1290	PIPE14X0.375
8	W14X38	W16X57	2258	PIPE16X0.500
7	W14X145	W16X77	3226	PIPE16X0.500
6	W14X145	W16X77	4194	PIPE20X0.625
5	W14X211	W16X89	4516	PIPE20X0.625
4	W14X211	W16X89	5161	PIPE22X0.625
3	W14X283	W16X89	5161	PIPE22X0.625
2	W14X283	W16X100	5484	PIPE22X0.625
1	W14X283	W16X100	5484	PIPE22X0.625

Selected members for 9-story Diagonal BRBF.

Story	Braced bay column	Braced bay Beam	BRB Core Area (mm^2)	Elastic Pipe (RL-BRB only)
9	W14X38	W12X35	968	PIPE10X0.500
8	W14X38	W12X35	1935	PIPE14X0.500

(continued on next column)

(continued)

Selected members for 4-story Chevron BRBF.

7	W14X74	W12X36	2581	PIPE16X0.625
6	W14X74	W16X36	3226	PIPE20X0.500
5	W14X145	W16X36	3548	PIPE20X0.500
4	W14X145	W16X36	3871	PIPE20X0.625
3	W14X211	W16X45	4194	PIPE20X0.625
2	W14X211	W16X45	4516	PIPE20X0.625
1	W14X211	W16X45	4516	PIPE20X0.625

Selected members for 12-story Chevron BRBF.

Story	Braced bay column	Braced bay Beam	BRB Core Area (mm^2)	Elastic Pipe (RL-BRB only)
12	W14X61	W16X26	1290	PIPE14X0.375
11	W14X61	W16X26	2258	PIPE20X0.500
10	W14X61	W16X26	2903	PIPE20X0.625
9	W14X145	W16X31	3871	PIPE20X0.625
8	W14X145	W16X31	4516	PIPE22X0.625
7	W14X145	W16X40	4839	PIPE22X0.625
6	W14X257	W16X40	5161	PIPE22X0.625
5	W14X257	W16X40	5806	PIPE24X0.625
4	W14X257	W16X40	5806	PIPE24X0.625
3	W14X370	W16X45	6452	PIPE24X0.625
2	W14X370	W16X45	6452	PIPE24X0.625
1	W14X370	W16X45	6452	PIPE24X0.625

Selected members for 12-story Diagonal BRBF.

Story	Braced bay column	Braced bay Beam	BRB Core Area (mm^2)	Elastic Pipe (RL-BRB only)
12	W14X61	W16X26	968	PIPE10X0.500
11	W14X61	W16X26	1613	PIPE16X0.500
10	W14X61	W16X26	3226	PIPE20X0.500
9	W14X120	W16X36	3548	PIPE20X0.625
8	W14X120	W16X36	4194	PIPE20X0.625
7	W14X120	W16X36	4194	PIPE20X0.625
6	W14X211	W16X45	4516	PIPE20X0.625
5	W14X211	W16X45	4839	PIPE22X0.625
4	W14X211	W16X45	4839	PIPE22X0.625
3	W14X311	W16X50	5484	PIPE22X0.625
2	W14X311	W16X50	5484	PIPE22X0.625
1	W14X311	W16X50	5484	PIPE22X0.625

CRediT authorship contribution statement

Milad Ehteshami Mocini: Writing – review & editing, Writing – original draft, Visualization, Validation, Supervision, Software, Resources, Project administration, Methodology, Investigation, Funding acquisition, Formal analysis, Data curation, Conceptualization. **S. Ali Razavi:** Writing – review & editing, Writing – original draft, Visualization, Validation, Supervision, Software, Resources, Project administration, Methodology, Investigation, Funding acquisition, Formal analysis, Data curation, Conceptualization.

Declaration of Competing Interest

The authors declare that they have no known competing financial interests or personal relationships that could have appeared to influence the work reported in this paper.

References

[1] AISC-341. Seismic Provisions for Structural Steel Buildings. American Institute of Steel Construction; 2016.
[2] Sen AD, Swatosh MA, Ballard R, Sloat D, Johnson MM, Roeder CW, et al. Development and evaluation of seismic retrofit alternatives for older concentrically braced frames. J Struct Eng 2016;143.
[3] Watanabe A., Hitomi Y., Saeki E., Wada A., Fujimoto M. Properties of brace encased in buckling-restraining concrete and steel tube. 9th World Conference on Earthquake Engineering. Tokyo-Kyoto, Japan 1988.
[4] Avci-Karatas C, Celik OC, Yalcin C. Experimental investigation of aluminum alloy and steel core buckling restrained braces (BRBs). Int J Steel Struct 2018;18:650–73.
[5] Bozorgnia Y, Bertero VV. From Engineering Seismology to Performance-Based Engineering. CRC Press; 2004.

[6] Wada A, Connor JJ, Kawai H, Iwata M, Watanabe A. Damage tolerant structures. 5th US-Japan Workshop on the Improvement of Structural Design and Construction Practices. ATC-15-4. San Diego, CA: Applied Technology Council; 1992. p. 27–39. ATC-15-4.
[7] Brown A.P., Aiken I.D., Jafarzadeh F.J. Buckling restrained braces provide the key to the seismic retrofit of the Wallace F. Bennett Federal Building. Modern Steel Construction 2001. p. 29–37.
[8] Tremblay R., Degrange G., Blouin J. Seismic rehabilitation of a four-storey building with a stiffened bracing system. 8th Canadian Conference on Earthquake Engineering. Vancouver-Canada 1999. p. 549-54.
[9] Tremblay R., Poncet L., Bolduc P., Neville R., DeVall R. Testing and design of buckling restrained braces for Canadian application. 13th World Conference on Earthquake Engineering. Vancouver, B.C., Canada 2004.
[10] Kazemi F, Jankowski R. Seismic performance evaluation of steel buckling-restrained braced frames including SMA materials. J Constr Steel Res 2023;201:107750.
[11] Mohebi B, Sartipi M, Kazemi F. Enhancing seismic performance of buckling-restrained brace frames equipped with innovative bracing systems. Arch Civ Mech Eng 2023;23:243.
[12] Asgarkhani N, Kazemi F, Jakubczyk-Gałczyńska A, Mohebi B, Jankowski R. Seismic response and performance prediction of steel buckling-restrained braced frames using machine-learning methods. Eng Appl Artif Intell 2024;128:107388.
[13] Asgarkhani N, Yakhchalian M, Mohebi B. Evaluation of approximate methods for estimating residual drift demands in BRBFs. Eng Struct 2020;224:110849.
[14] Yakhchalian M, Asgarkhani N, Yakhchalian M. Evaluation of deflection amplification factor for steel buckling restrained braced frames. J Build Eng 2020;30:101228.
[15] Fahnestock LA, Sause R, Ricles JM. Seismic response and performance of buckling-restrained braced frames. J Struct Eng 2007;133:1195–204.
[16] Tremblay R, Merzouq S. Dual Buckling Restrained Braced Steel Frames for Enhanced SeismicResponse. Passive Control Symposium. Tokyo Institute of Technology; 2004. p. 89–104.
[17] Mehdipanah A, Mirghaderi SR, Razavi SA. Seismic performance of stiffness-based designed buckling-restrained braced frame and special moment-resisting frame dual systems. Struct Infrastruct Eng 2015;12.
[18] Razavi S.A., Shemshadian M.E., Mirghaderi S.R., Ahlehagh S. Seismic design of buckling restrained braced frames with reduced core length. Structural Engineering World Congress. Italy 2011.
[19] Zaruma S, Fahnestock LA. Assessment of design parameters influencing seismic collapse performance of buckling-restrained braced frames. Soil Dyn Earthq Eng 2018;113:35–46.
[20] Razavi SA, Mirghaderi SR, Hosseini A. Experimental and numerical developing of reduced length buck-ling-restrained braces. Eng Struct 2014;77:144–60.
[21] Dizaj Fanaei N. EA. Response modification factor of the frames braced with reduced yielding segment BRB. Struct Eng Mech 2014;50:1–17.
[22] Estekanchi HE, Valamanesh V, Vafaei A. Application of endurance time method in linear seismic analysis. Eng Struct 2007;29:2551–62.
[23] ASCE-7. Minimum Design Loads and Associated Criteria for Buildings and Other Structures. American Society of Civil Engineers; 2016.
[24] AISC-360. Specification for Structural Steel Buildings. American Institution of Steel Construction; 2016.
[25] Seismosoft. SeismoStruct, User manual. In: Ltd S, editor. 2018.
[26] Ibarra LF, Medina RA, Krawinkler H. Hysteretic models that incorporate strength and stiffness deterioration. Earthq Eng Structrual Dyn 2005;34:1489–511.
[27] Lignos DG, Krawinkler H. Deterioration modeling of steel components in support of collapse prediction of steel moment frames under earthquake loading. J Struct Eng 2011;137:1291–302.
[28] Eryasar ME, Topkaya C. Experimental and numerical investigation of buckling restrained braces. Ankara, Turkey: Middle East Technical University; 2009.
[29] FEMA(P-695). Evaluation of the FEMA P-695 Methodology Quantification of Building Seismic Performance Factors. NEHRP Consultants Joint Venture; 2010.
[30] Uang CM. Establishing R (or Rw) and Cd factors for building seismic provisions. J Struct Eng 1991;117:19–28.
[31] Homayoon E. Estekanchi a MMa, Hassan Vafai b, Goodarz Ahmadi c, Sayyed Ali Mirfarhadi a, Mojtaba Harati d. A state-of-knowledge review on the endurance time method. Structures. 27:2288-2299.
[32] Mirfarhadi SA, Estekanchi HE. Value based seismic design of structures using performance assessment by the endurance time method. Struct Infrastruct Eng 2020;16.
[33] Rahimi E, Estekanchi HE. Collapse assessment of steel moment frames using endurance time method. Earthq Eng Eng Vib 2015;14:347–60.
[34] Mirzaee A, Estekanchi HE. Performance-based seismic retrofitting of steel frames by the endurance time method. Earthq Spectra 2015;31:383–402.
[35] Hariri-Ardebili MA, Sattar S, Estekanchi HE. Performance-based seismic assessment of steel frames using endurance time analysis. Eng Struct 2014;69:216–34.
[36] Amiri HA, Estekanchi HE. Life cycle cost-based optimization framework for seismic design and target safety quantification of dual steel buildings with buckling-restrained braces. Earthq Eng Struct Dyn 2023;52:4048–81.
[37] Mohsenian V, Hajirasouliha I, Nikkhoo A. Multi-level response modification factor estimation for steel moment-resisting frames using. J Earthq Eng 2020;26:4812–32.
[38] Dehghani M, Tremblay R. Design and full-scale experimental evaluation of a seismically endurant steel buckling-restrained brace system. Earthq Eng Struct Dyn 2017;47:105–29.
[39] Eryaşar ME, Topkaya C. An experimental study on steel-encased buckling-restrained. Earthq Eng Struct Dyn 2010;39:561–81.
[40] Razavi S, Kianmehr A, Hosseini A, Mirghaderi R. Buckling-restrained brace with CFRP encasing: mechanical behavior & cyclic response. Steel Compos Struct 2018;27:675–89.